An All-Digital High-Performance Drive System for Linear Permanent Magnet Synchronous Motor

Michael S.W. Tam, Norbert C. Cheung

Power Electronics Research Centre,
Department of Electrical Engineering,
Hong Kong Polytechnic University
Hunghom, Kowloon, Hong Kong SAR.

Abstract - Permanent magnet motors are used in a wide variety of applications. Their use has increased following the availability of the new high flux Neodymium-Iron-Boron magnets. Permanent Magnet Synchronous Motor (PMSM) has the advantages of high thrust density. It is also inherently more robust & maintenance free. In the application of linear motion, the Linear Permanent Magnet Synchronous Motor (LPMSM) has some further advantages that it can reduce the mechanical parts and allows a more simple & reliable motion system. Together with the advance of microelectronics, there is a trend that the LPMSM will continue to replace the traditional DC Brush Motor & lead screw linear motion system. [1], [2]

In this project, a full-digital driver will be developed for the application of LPMSM. The driving system will then be used as high precision & high-speed applications such as die-bonding and wire-bonding.

1. Introduction

Permanent magnet motors are used in a wide variety of applications. Their use has increased following the availability of the new high flux Neodymium-Iron-Boron magnets.

Around the various types of PM motors, the brushless type PM Synchronous Motor (PMSM) becoming an important stream. They are used for computer hard & floppy disc drives; about 10 million are produced each year. In industry, they are used in servo drives for machine tools such as X-Y table, bond head actuator & robotic arm.

In the application where linear motion is required, the Linear Permanent Magnet Synchronous Motor (LPMSM) has particular advantages. As the LPMSM is used the traditional mechanical coupler, rotary bearings and the costly lead-screw can be eliminated. Besides, the LPMSM utilize high-energy product magnets and are characterized by high thrust density, low losses, small electrical time constant and rapid responses. Furthermore, like the rotary PMSMs, the LPMSMs are brushless, this imply the motor has a higher efficiency, reduce EMI generation and require no maintenance on the brushes of the motor. Hence there is no deterioration of performance over the life of the motor. [4], [10].

For travel of longer than 20mm, LPMSMs are generally in the form of multi-phase, which require the fed through of power electronic controller for commutation. Thanks to the advance of microelectronics, regenerative electric braking can be taken as an advantage of the LPMSM that allow a high-speed, high precision, large-thrust and high robustness to be implemented. [1]

This paper is divided into 3 stages:

(i) Develop a full-digital drive under conventional driving method
(ii) Investigate the high performance driving scheme that is suitable for high speed & high precision applications
(iii) Hardware implementation of the driving scheme and verify the performance.

Fig. 1 shows the photo of the Linear Permanent Magnet Synchronous Motor. The upper right corner is the digital drive.

Fig. 1 A Linear Permanent Magnet Synchronous Motor

2. The LPMSM Driver

The LPMSMs are of brushless type motors; therefore another electronic means of commutation (AC driving) is needed when controlling the motor.

With the continual advancement of microelectronics, powerful electronic devices and micro controller units, such as the IGBT power drivers & DSP processors, are readily available. This allows the building of the high efficient digital driver at a very competitive cost and high performance. In addition, the complexity associates with controlling an ac drive are readily being overcome. [9]

With a suitable control methodology, ac drives are superior than dc drives in high performance applications.

The gradual replacement of dc drive has begun and ac drives can be expected to continue to overtake them over the next decade. It is still too early to determine if dc drives will eventually be relegated to the history book as have nearly all other commutated machines such as rotary converters, amplidynes and the like. However, the next decade will surely witness a marked increase in the use of ac drive. [10]

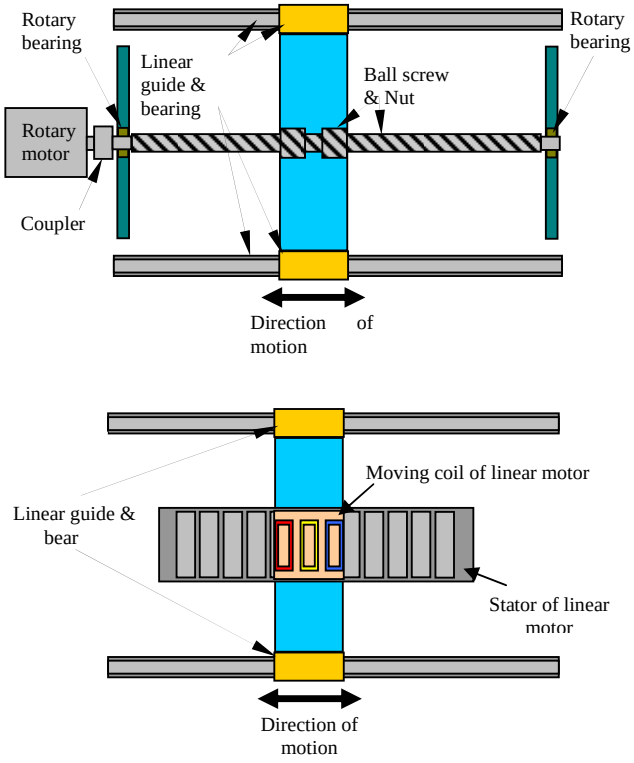

Fig. 2 Comparing the traditional drive with the LPMSLM

The objective of the project is to derive an efficient, robust and low-cost digital driver for the LPMSM that is suitable in the application of high speed & high precision motion control system.

The tradition linear motion system driven by the rotary motor is shown in the upper part of Fig. 2. Comparing to the Linear Permanent Magnet Synchronous Motor in the lower portion of Fig. 2, the following components can be eliminated:

(a) The rotary bearing,
(b) The mechanical coupler
(c) The ball-screw & nut
(d) The extra rotary encoder for the commutation control and position control of the motor.

Therefore the resulting driving system consists of less mechanical parts and this has made the design more simple, straightforward and less costly. In practice, for a 5μm accuracy 6"x6" X-Y table, cost reduction of up to 80% is possible with the replacement of the rotary system by the linear one. Besides the overall mechanical friction in the system is a lot smaller, less audible noise will be generated and the motor can move faster. In addition, the position sensor is attached very close to the load; the position of the load can be more accurate. Furthermore, the system is virtually free of maintenance and this means a more robust and reliable motion system is possible.

3. Modelling of the Linear PMSM

Refer to the magnetic circuit in the diagram to the right below, the magnetic potential F, flux density B and the flux ϕ is given by the following equations:

$$F = \oint H\,dl = \sum NI$$

$$B = \mu_o H$$

$$\phi = \int B\,dS$$

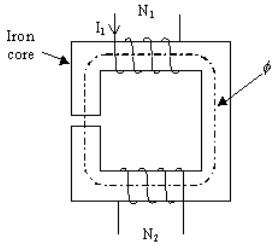

$\lambda_1 = N_1 \phi \Rightarrow L_{11} = \lambda_1/I_1$
$\lambda_2 = N_2 \phi \Rightarrow L_{12} = \lambda_2/I_1$
where : H is the magnetizing force
N is the number of turn
B is the magnetic flux density
μ_o is the permeability of air
ϕ is the magnetic flux
λ_1, λ_2 are the magnetic flux linkage to coil N_1, N_2 respectively

Fig. 3 The magnetic structure of the LPMSM

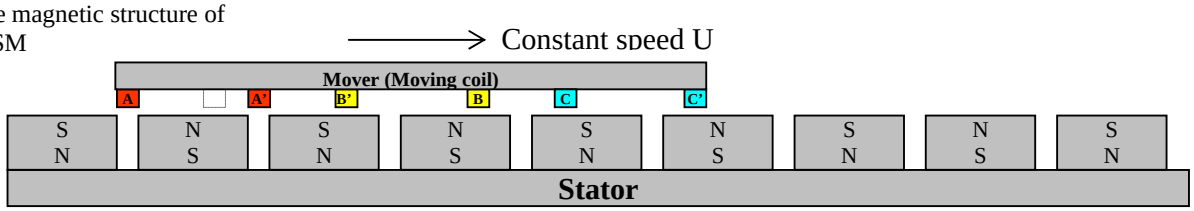

Fig. 3 is the structure of a LPMSM in the cross-sectional view. The stator is a series of magnet stick on a ferro-magnetic material, usually made of soft iron. The magnetic axis of the magnet is mounted vertically while the sequence of the magnets is alternating in the way NS, SN, and NS … etc.

Due to the fringing effect, and by a suitably design the size, the spacing of the magnets and the choice of the distance above the magnets, a sinusoidal distributed magnetic flux can be obtained along the horizontal position (x).

The LPMSM can be in the form of moving coil or moving magnet. For long travel, moving coil is preferable, as the inductance of the coil can be kept to minimum. While for short distance, moving magnet can help to save the costly magnet. The LPMSM as shown in the Fig. 3 is a moving coil one. [1] Separate winding instead of lap winding is used in this motor. Such arrangement helps ease the production of the winding coils. As the coils are identical, they can be mass-produced and glued to the mounting plate.

Refer to Fig. 3, if the magnetic pole pitch is p, and the coils are moving at a speed u, then the distance x move in t is:

$$x = ut \quad \text{.....(3.2.1)}$$

The corresponding magnetic angle θ is:

$$\theta = \frac{x}{p} \quad \text{.....(3.2.2)}$$

Assume the magnetic flux linking the coils is sinusoidal distributed along the position x-axis under concern; with a maximum magnetic flux density of Φ, the magnetic flux density function is thus:

$$\theta = \frac{ut}{p} \quad \text{.....(3.2.3)}$$

$$\phi = \Phi \sin\left(\frac{ut}{p}\right) \quad \text{..... ....(3.2 .4)}$$

The EMF induced e_A in the winding of phase A is the rate of change of the total flux linkage λ:

$$e_A = \frac{d\lambda}{dt} \quad \text{.....(3.2.5)}$$

$$e_A = 2Nl\frac{d\phi}{dt} = 2Nl\frac{d\sin\left(\frac{ut}{p}\right)}{dt} = 2Nl\frac{u}{p}\cos\left(\frac{ut}{p}\right) \quad \text{..... ....(3 .2.6)}$$

Where N is the number of turns of the winding
l is the length of the winding orthogonal to the motion

The induced emf of winding B & C are the same as winding A, except that they are 2π/3 phase lag & lead to winding A respectively i.e.:

$$e_B = 2Nl\frac{u}{p}\cos\left(\frac{ut}{p} - \frac{3\pi}{2}\right) \quad \text{..... ....(3.2.7)}$$

$$e_C = 2Nl\frac{u}{p}\cos\left(\frac{ut}{p} + \frac{3\pi}{2}\right) \quad \text{..... ....(3.2.8)}$$

As the coils are separated from each other, assume the mutual inductances between the windings are negligible. The system equations in matrix form is thus:

$$\begin{bmatrix} v_a \\ v_b \\ v_c \end{bmatrix} = \begin{bmatrix} R_a & 0 & 0 \\ 0 & R_b & 0 \\ 0 & 0 & R_c \end{bmatrix}\begin{bmatrix} i_a \\ i_b \\ i_c \end{bmatrix} + \frac{d}{dt}\begin{bmatrix} L_{aa} & 0 & 0 \\ 0 & L_{bb} & 0 \\ 0 & 0 & L_{cc} \end{bmatrix}\begin{bmatrix} i_a \\ i_b \\ i_c \end{bmatrix} + \begin{bmatrix} e_a \\ e_b \\ e_c \end{bmatrix} \quad \text{.....(3.2. 9)}$$

Putting eqn3.2.6-8 in to eqn3.2.9,

$$\begin{bmatrix} v_a \\ v_b \\ v_c \end{bmatrix} = \begin{bmatrix} R_a & 0 & 0 \\ 0 & R_b & 0 \\ 0 & 0 & R_c \end{bmatrix}\begin{bmatrix} i_a \\ i_b \\ i_c \end{bmatrix} + \frac{d}{dt}\begin{bmatrix} L_{aa} & 0 & 0 \\ 0 & L_{bb} & 0 \\ 0 & 0 & L_{cc} \end{bmatrix}\begin{bmatrix} i_a \\ i_b \\ i_c \end{bmatrix} + 2Nl\frac{u}{p}\begin{bmatrix} \cos\left(\frac{ut}{p}\right) \\ \cos\left(\frac{ut}{p} - \frac{3\pi}{2}\right) \\ \cos\left(\frac{ut}{p} + \frac{3\pi}{2}\right) \end{bmatrix} \quad \text{.....(3.2. 10)}$$

v_A, v_B & v_C are the voltage across the phase windings
i_A, i_B & i_C are the current flow in the phase windings
R_A, R_B & R_C are the resistance of the phase windings
L_A, L_B & L_C are the self-inductance of the phase windings

Since the 3 phase windings are identical, their resistance & inductance are the same and are equal to R & L respectively. The term *2Nl/p* is the emf constant of the motor and it can equate to K_e. Therefore the LPMSM system equations of (3.2.10) can be re-written as:

$$\begin{bmatrix} v_a \\ v_b \\ v_c \end{bmatrix} = \begin{bmatrix} R & 0 & 0 \\ 0 & R & 0 \\ 0 & 0 & R \end{bmatrix} \begin{bmatrix} i_a \\ i_b \\ i_c \end{bmatrix} + \frac{d}{dt} \begin{bmatrix} L & 0 & 0 \\ 0 & L & 0 \\ 0 & 0 & L \end{bmatrix} \begin{bmatrix} i_a \\ i_b \\ i_c \end{bmatrix} + K_e u \begin{bmatrix} \cos\left(\frac{ut}{p}\right) \\ \cos\left(\frac{ut}{p} - \frac{3\pi}{2}\right) \\ \cos\left(\frac{ut}{p} + \frac{3\pi}{2}\right) \end{bmatrix} \quad .....(3.2.11)$$

Assume 100% electro-mechanical energy transfer, the thrust force produced by the motor is:

$$F_e = \frac{1}{u}(i_a e_a + i_b e_b + i_c e_c) \quad .....(3.2.12)$$

Taking into account the frictional force F_F , the mover's inertia M_M , the cogging force F_C and the load F_L, the mechanical force output is:

$$F_M = M_M \frac{d}{dt} u + B u + F_L + F_C \quad .....(3.2.13)$$

Where B is the frictional constant

3. Implementation of the Digital LPMSM driver

Fig. 4 shows the switching devices arrangement of the 3-phase bridge. It consists of 3 high-side and low-side half bridges connected in parallel. A diode is connected across to each switch. [4], [9]
The timing of the switching sequence for the 3-phase bridge is shown in Fig4.1.2 on the next page.
It is a 6-step switching sequence that the high and low side of the switching devices are switched on & off respectively in a cycle. While the other 2 high low side branches are switched on and off with 120° phase shift.

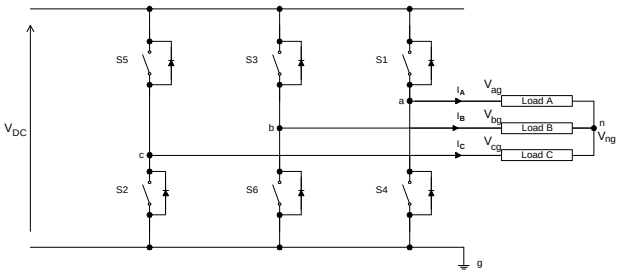

Fig. 4 The three phase full bridge MOSFET

Since the switching signals are sinusoid modulated PWM, the resulting voltage waveforms will be sinusoidal. In doing so, a 3-phase voltage with variable frequency & amplitude can be obtained. Then by feeding back the current signal and PD controlling the current loop, a current controlled (or torque controlled) 3-phase PWM driver can be obtained.

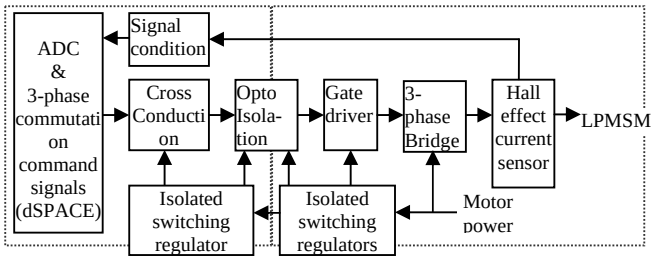

Fig. 5 Block Diagram for the LPMSM Driver

Fig. 5 is the block diagram of the Digital LPMSM driver. The current sensors are 2 Hall-Effect devices for detecting up to ±10A current. The analog hall-sensor outputs are conditioned and fed into the ADC of the dSPACE card. The 3rd current is calculated in the dSPACE card by using: $I_3 = -(I_1 + I_2)$.

The 3-phase bridges are 3 pairs of high-low side power MOSFET half-bridges. In considering the actual application in a X-Y table of a wire-bonder machine, power rating will be around 5A to 10A @ 100V, select the power MOSFET IFR640 with power handling capability of 18A 200V (100% safe margin). The bridges are pre-driven by IC gate-drivers with 100% duty cycle driving ability. The motor side & logic side is electrically isolated by the opto-couplers that may introduce about 300nS delay. A PAL is written for protection against the cross conduction of the high-low side MOSFET. The signal command for the 3-phase bridge is from the PC through the dSPACE card.

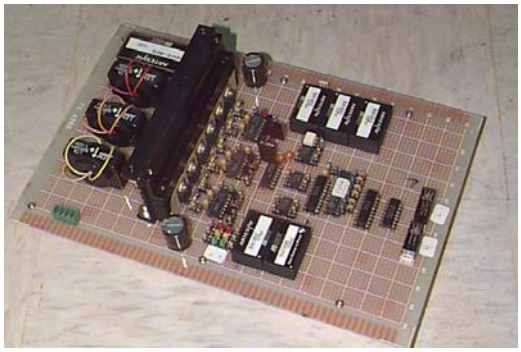

Fig. 6 Photo of the LPMSM driver

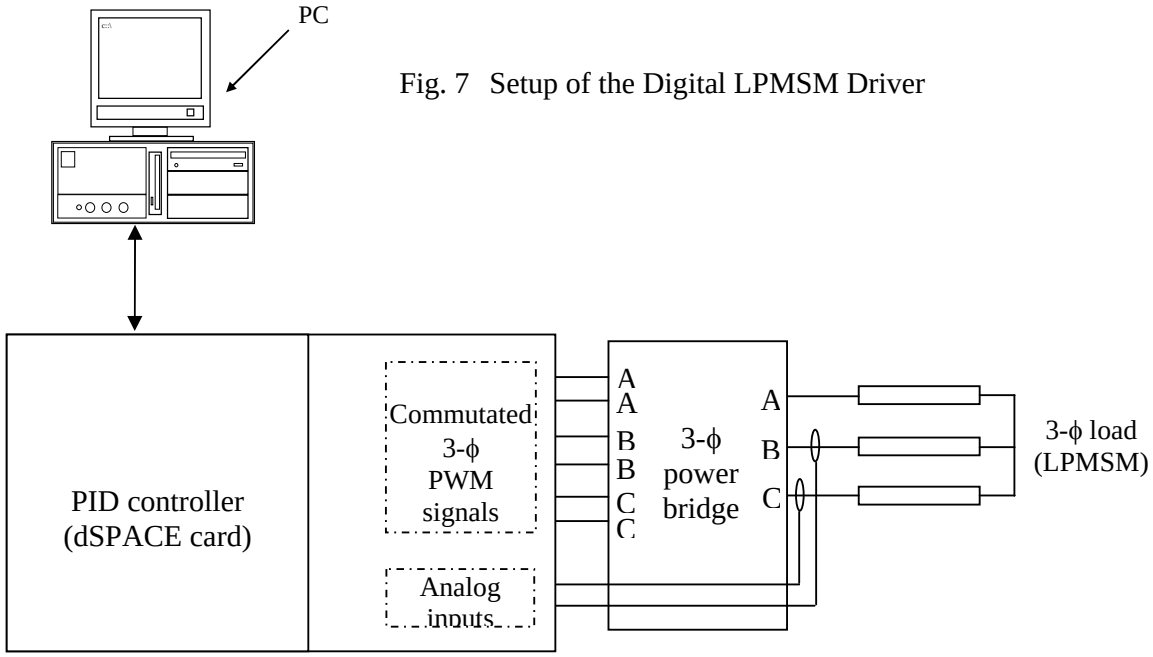

Fig. 7 Setup of the Digital LPMSM Driver

The arrangement of the parts for the digital LPMSM driver is shown in the Fig 7. It consists of a PC for editing, compiling, monitoring & downloading the program into the dSPACE card. The dSPACE card is the controller that contains a DSP, IO, PWM outputs & Analog input for controlling the 3-phase driver. The 3-phase driver is for delivering power to the linear motor whose current is to be controlled.

4. The PID Controller

At this stage, the PID control algorithm is used in the position control loop. Since it is familiar to us it allows a quick start up of the project. Also the result can be used as comparison.

For the LPMSM drive a direct drive system, it is relative sensitive to the load changing. Some adaptive control schemes are investigated and analyzed to find a best suit for the system.

The inner loop has the highest bandwidth is the current loop which is the implemented by the digital driver. The force output from the LPMSM is proportional to the motor current. The second loop and the outer loop can be done in the controller at the same time, as the velocity signal is the derivative of the position signal.

The system has a hierarchical structure in bandwidth that the external loop has the lowest frequency response. Such topology allows the design of each loop separately. The control algorithm for the controller1, 2 & 3 are P, PI & PID respectively.

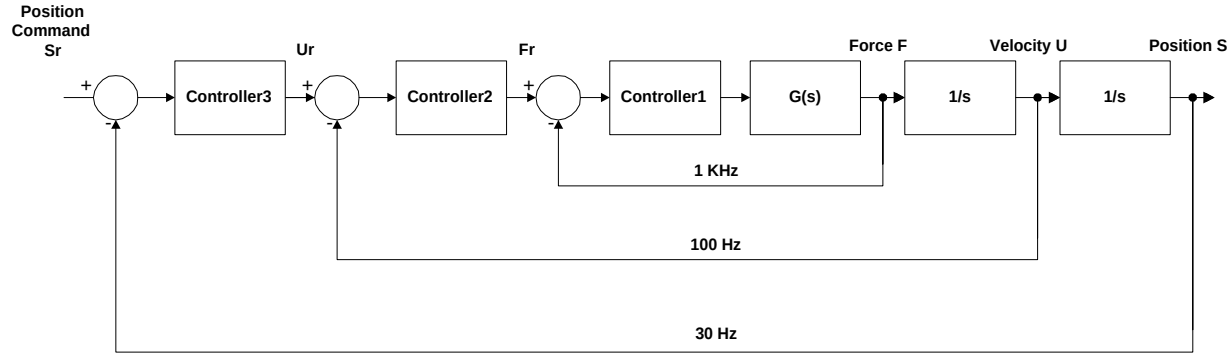

Fig. 7 The control strategy

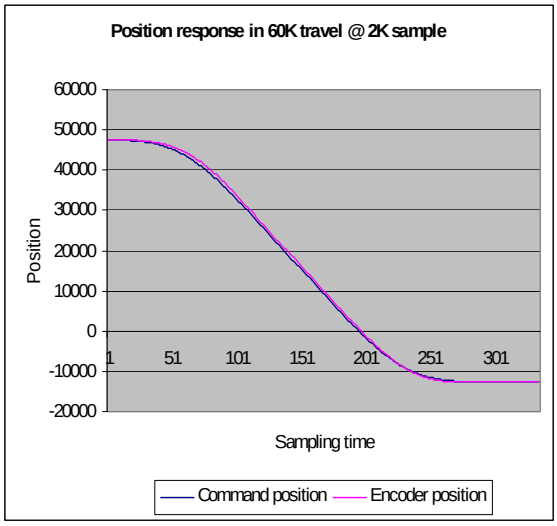

Fig. 13. 60mm point-to-point travel using a third order profile

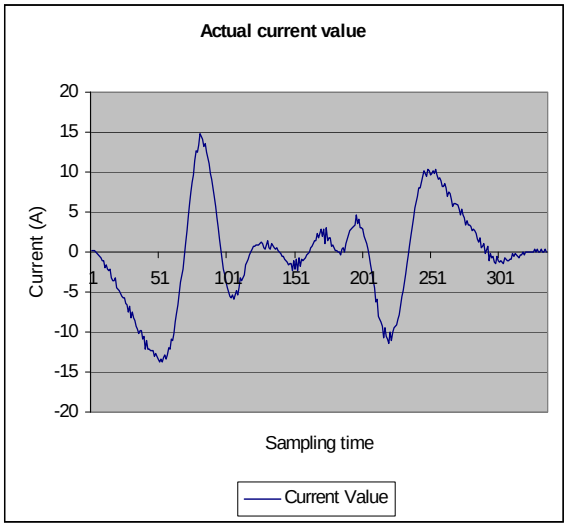

Fig. 14. Actual current waveform for the 60mm travel

5. Result of Hardware Implementation

Fig. 13 and Fig. 14 are the responses of the position loop. The sampling frequency for the current loop and position loop is 10KHz and 2KHz respectively. A third order profile is used to generate the position command signal for a better position tracking and minimize the stress on the current driver and the motor. As shown in the results, the driver can control the motor to track the command profile with very high precision.

5. Conclusion

This paper describes the development of a linear drive system with high-acceleration/deceleration and high accuracy performances. A fully digital PWM circuit that supplies momentary over-rated current to the LPMSM is constructed. A dual rate multi-loop cascade controller with velocity/acceleration feedforward and velocity observer is proposed. The overall system is simulated and implemented in hardware. Both simulated results and implementation measurements show that the current controller has a fast current loop response and good current tracking ability. The current loop has bandwidth of 1.5KHz and a driving capacity of 25A peak current at 150Vdc. The digital current driver exhibits very low temperature-drift (20mA max.) and offset-drift (5mA max.). The system has the ability to drive the linear motor at a speed of 4m/s, a peak acceleration of 5G, and a position error of 1 micron. The developed linear drive system is very suitable for deployment in next-generartion of high-performance electronic packaging machines.

6. Acknowledgment

The author would like to thank the Research Grants Council for the funding of this research work through the Competitive Earmarked Research grant PolyU5100/99E.

7. References

[1] I.Boldea & Syed A. Nasar, "Linear Electric Actuators & Generators", Cambridge University Press, 1997

[2] Mulukutla S. Sarma, "Electric Machine – Steady State Theory & Dynamic Performance", West Publishing Company, 1994

[3] Dal Y. Ohm, "Control & Application of AC Servo Motors", 26th Annual Symposium on Incremental Motion Control Systems & Devices, July1997

[4] I.Boldea & S.A. Nasar, "Vector Control of AC Drives", CRC Press Inc, 1992

[5] Shahian/Hassul, " Control System Design Using Matlab", Prentice-Hall, 1993

[6] J.S. Ko, J.H. Lee, M.J. Youn, "Robust digital position control of brushless DC motor with adaptive load torque observer" IEE Proc.-Electr. Power Appl., Vol.141,No.2, Mar1994

[7] J. Hu, D.M. Dawson, K. Anderson, "Position Control of a brushless DC motor without velocity measurement", IEE Proc.-Electr. Power Appl., Vol.142, No.2, Mar1995

[8] F.J. Lin, K.K. Shyu, Y.S. Lin, "Variable structure adaptive control for PM synchronous motor drive", IEE Proc.-Electr. Power Appl., Vol.146,No.2, Mar1999

[9] Y. Dote, "Servo Motor & Motion Control Using Digital Signal Processing", Prentice Hall 1990

[10] J.D.V. Wyk, "Power electronic converters for motion control", Proceeding of the IEEE, pp1194-1214, Aug1994